The Nature of the Interactions between Pt_4 Cluster and the Adsorbates $^{\cdot}H$, $^{\cdot}OH$, and H_2O

Renato L. T. Parreira,*,† Giovanni F. Caramori,‡ Sérgio E. Galembeck,† and Fritz Huguenin†

Departamento de Química, Faculdade de Filosofia, Ciências e Letras de Ribeirão Preto, Universidade de São Paulo, Avenida Bandeirantes 3900, 14040-901, Ribeirão Preto, SP, Brazil, and Departamento de Química Fundamental, Instituto de Química, Universidade de São Paulo, Avenida Prof. Lineu Prestes 748, Bl. 05 sup. Sl 555, Butantã, 05508-000, São Paulo, SP, Brazil

Received: April 16, 2008; Revised Manuscript Received: July 25, 2008

The nature of the interactions between the platinum cluster Pt_4 and the adsorbates $^{\cdot}H$, $^{\cdot}OH$, and H_2O, as well as the influence of these adsorbates on the electronic structure of the Pt_4 cluster, was investigated by density functional theory (B3LYP, B3PW91, and BP86) together with the effective core potential MWB for the platinum atoms, and 6-311++G(d,p) and aug-cc-pVTZ basis set for the H and O atoms. Identification of the optimal spin multiplicity state and the preferential adsorption sites were also evaluated. Adsorption changes the cluster geometry significantly, but the relaxation effects on the adsorption energy are negligible. The adsorbates bind preferentially atop of the cluster, where high bonding energies were observed for the radical species. Adsorption is followed by a charge transfer from the Pt_4 cluster toward radical adsorbates, but this charge transfer occurs in a reversed way when the adsorbate is H_2O. In contrast with water, adsorption of the radicals $^{\cdot}H$ and $^{\cdot}OH$ on platinum causes a remarkable re-distribution of the spin density, characterized by a spin density sharing between the $^{\cdot}H$ and $^{\cdot}OH$ radicals and the cluster. The covalent character of the cluster−adsorbate interactions, determined by electron density topological analysis, reveals that the Pt_4−H interaction is completely covalent, Pt_4−OH is partially covalent, and Pt_4−H_2O is almost noncovalent.

1. Introduction

The electronic portable equipment industry has shown great interest in developing high energy density sources, enabling the fabrication of devices with reduced dimensions and a large number of functions and long operation time. Therefore, the current trend is to miniaturize and improve the efficiency of these energy sources, e.g., the fuel cells, which convert the chemical energy of fuels such as hydrogen, alcohols, and hydrocarbons into electric energy.[1] In these sorts of cells, the fuel and oxygen are added continuously, thus avoiding the exhaustibility and interruption of the operation, typically observed for primary and secondary batteries. Particularly, methanol and ethanol are frequently employed as fuels due to their easy availability and low cost. Therefore, there has been a growing interest in minicells and fuel cells such as the direct methanol fuel cells (DMFC) and the direct ethanol fuel cells (DEFC), which are suitable as energy sources in means of transport and portable electronic devices due to their high energy density, low noise, and easy maintenance.[2−6] DMFC and DEFC offer further advantages compared with hydrogen/oxygen fuel cells, since the latter have limited use because of transportation and storage difficulties.[7] On the other hand, a catalytic reform is necessary to perform the extraction of molecular hydrogen from liquid fuels.[7]

Nanoparticles from noble metals have been applied to improve the efficiency of fuel cells and reduce the costs involved in their production. Among the transition metals, platinum is extensively applied in heterogeneous catalytic processes because of its high catalytic activity and chemical and thermal stabilities.[8−14] The electrooxidation of methanol under platinum (or under PtM alloys, usually PtRu)[15] is rather tough, leading to complicated heterogeneous structures that involve electrocatalysts, either the anode or the cathode.[15,16] During the process of oxygen electroreduction in acidic medium, a large assortment of intermediates can be present; e.g., atomic oxygen, H_2O_2, H_2O, OH, and OOH radicals, among others.[17,18] Despite the high efficiency of platinum in the anodic dehydrogenation of hydrocarbons and alcohols, its surface can be easily poisoned with carbon monoxide, which limits reaction rates.[6,8] In aqueous medium, water can oxidize the carbon monoxide through a reaction between the latter and the adsorbed OH radical, thus minimizing but not eliminating the blocking effects of carbon monoxide at moderate potentials.[6,8] At a first glance, the formation of water on the platinum surface seems to happen in a very simple way (in contact with the platinum surface, hydrogen and oxygen react at room temperature, yielding water).[19] However, the proposed mechanism and stoichiometry of the disproportionation reaction of O and H_2O and the formation of the OH radical are still contradictory.[20,21] In general, after O_2 dissociation, atomic oxygen can react with atomic hydrogen through two different pathways: (i) above the desorption temperature of water, hydrogen reacts with oxygen, producing water, which desorbs from the platinum surface; (ii) below the desorption temperature, water participates actively by reacting with atomic oxygen, thus producing the hydroxyl radical.[21] A good review of this topic can be found in a study about the catalytic formation of water on the platinum surface by Michaelides and Hu.[19] In this way, studies regarding adsorption properties and reactions of several adsorbates (intermediates in catalytic processes) such as $^{\cdot}H$, O, $^{\cdot}OH$, H_2O, CO, CH_n, and smaller oxygenated organic molecules on the platinum surface are not only fundamental to a better understanding of the reaction mechanisms involved in heterogeneous

* To whom correspondence should be addressed. Tel.: +55 16 3602-4862. Fax: +55 16 3633-8151. E-mail: rtame@usp.br/rtame77@yahoo.com.br.

† Departamento de Química, Faculdade de Filosofia, Ciências e Letras de Ribeirão Preto.

‡ Departamento de Química Fundamental, Instituto de Química.

10.1021/jp8033177 CCC: $40.75
Published on Web 10/23/2008

catalytic processes, but they also contribute to research such in fields as electrochemistry and corrosion.[18]

In the past years, different theoretical methods have been applied to the study of catalytic reactions on solid surfaces,[22−25] contributing to either the characterization or the improvement of the catalytic performance of adsorption sites.[26] Although theoretical approaches are important to establish catalytic mechanisms, there is some difficulty in describing chemisorption on platinum surfaces when they are employed mainly because of the large number of electronic states stemming from the occupation of 5d orbitals (unoccupied or not completely filled up).[9,14,27] In general, the computational strategies employed to give a quantum mechanical description of the surfaces can include approximations such slab/supercell or cluster-approximation, each one with its advantages and disadvantages.[14−23,27−29] The slab/supercell approximation has great applicability in studies involving ordered overlayers, but it is not adequate for highly dispersed catalysts. The cluster-approximation describes the effects of the local electronic structure in chemisorption processes, whereas the cluster must be chosen to reproduce the sites of chemical interest.[27,28] Despite the use of quantum chemistry methods to predict the interactions between adsorbates and catalytic sites, it is also necessary to make careful comparisons with experimental data, in order to determine what theory levels and strategies are reasonable to describe the active sites within an acceptable CPU time.[24,25,30]

Metallic clusters have been frequently employed as models of metallic surfaces in studies on the adsorption of individual species, yielding good results concerning the description of the surface reaction,[14,27,31,32] adsorbates structures, stretching frequencies, and chemisorption energies.[23,33−35] The use of clusters is related not only to the idea that adsorption and desorption reactions are processes localized in small defined sites of the catalyst particle (local phenomena) but also to the problems to perform ab initio calculations for large systems.[23,26,33,34] Transition metal clusters with intermediate size can also provide insights into the fundamental reaction mechanisms on the surface.[9,13,32] In addition, they constitute an excellent framework to perform systematic studies about the structure/properties relationships when the size of the cluster is increased.[11]

Up to date, experimental and theoretical studies have been fundamental when proposing reaction mechanisms and exploring aspects related to the thermochemistry of catalytic processes involving adsorbed species on platinum surfaces (or in PtM alloys). However, the nature of the cluster−adsorbate chemical bonding still attracts a lot of attention[27,28,36−39] and can contribute to clarifying a set of previously proposed mechanisms of catalytic processes involving platinum.[39] In this way, the goal of the present work is to investigate the nature of the cluster−adsorbate bonding and to verify how the structure of the cluster is affected by the adsorption. In particular, the bonding between the adsorbates (•H and •OH radicals, and H_2O molecule) and the tetrahedral Pt_4 cluster will be considered. This Pt_4 cluster model had been previously used as a model in different theoretical studies such as CO[40−42] and NO[43] adsorption, methane photodissociation,[41,44] interaction with H_2O, NH_3,[41,45] and O_2,[33] effect of particle size on O and S adsorption,[46] reaction with molecular hydrogen,[26,31] effects of the external electrical field on the stretching frequencies of adsorbed CO and OH^-,[34] influence of supports on chemisorption properties of hydrogen, oxygen,[47] and CH_n species[48] (under platinum). The above-mentioned studies have employed methodologies such as CASSCF (complete active space self-consistent field), DFT (density functional theory), and CI (configuration interaction). Recently, Pt_4 cluster has been employed as a model to study dehydrogenation[32] and methane activation.[49] So this work shall contribute to characterizing and shedding new light on the electronic effects that stem from the bonding between platinum cluster and some adsorbates, commonly found in heterogeneous catalytic processes within fuel cells. The nature of the cluster−adsorbate bonding and the changes in the geometric and electronic structure of the Pt_4 cluster were analyzed by means QTAIM (quantum theory of atoms in molecules) analysis, spin densities, stretching frequencies, charge-transfer effects, and molecular orbitals.

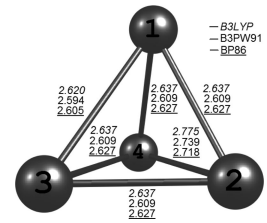

Figure 1. Bond lengths for Pt_4 (distorted tetrahedral, triplet).

2. Computational Methods

All geometry optimizations were carried out by using the Gaussian03 package[50] in conjunction with hybrid functionals such as B3LYP[51−53] and B3PW91[51,54−56] and the correlation functional BP86.[57,58] For the Pt atoms, the effective core potential (ECP) MWB (Stuttgart/Dresden double-ζ (SDD)[59−71] was employed, which includes 60 core electrons, relativistic contributions, and the valence basis set 8s7p6p for the primitive form and 6s5p3d for the contracted form. For the other atoms (H and O), two different basis set were employed; 6-311++G(d,p)[72−74] and aug-cc-pVTZ.[75] Geometry optimizations were refined by considering the options OPT=Tight and Int=Ultrafine. The first option employs the following convergence criteria: (i) Maximum Force=1.5×10^{-5}, (ii) rms Force=1.0×10^{-5}, (iii) Maximum Displacement=6.0×10^{-5}, (iv) rms Displacement=4.0×10^{-5}; the second one requires a more accurate integration grid [pruned (99 590) grid]. The nature of the stationary points was determined by performing the harmonic vibration analysis. To verify the effects of geometry relaxation on the adsorption energies and the interaction energies between the cluster and the adsorbates, geometry optimizations were carried out with and without symmetry constraints (the Pt−Pt distances were kept constant and equal to the experimental bulk, 2.775 Å).[76−78]The topological analysis of the electron density was performed by using the AIM (atoms in molecules) theory,[79−81] which has been largely employed to characterize different sorts of interactions in molecular complexes.[82] It was carried out by using the software suite programs AIMPAC.[83] The molecular orbitals were visualized by the Molekel 5.3 software.[84] The structures in Figure 1 were drawn with the Chemcraft Lite software.[85] Spatial orientation of the adsorbates were visualized by the Diamond demonstration version 3.1.[86]

3. Results and Discussion

Computational studies have described aspects related to the structure and energy of the metal−metal bonding, conformations, special arrangements resulting in different symmetries, electronic configuration, stabilities, conduction and valence bands, magnetic momenta, and different spin states for a large variety of platinum clusters, Pt_n.[9−13,27,31,33,41,43,87−99] The aim of the present paper is neither to reinvestigate the several stable

TABLE 1: Spin Multiplicity (SM), Atom (E_{elec}^{Pt}) and Cluster ($E_{elec}^{cluster}$) Electronic Energies, Zero Point Correction (ZPE), Electronic Energies Corrected by ZPE ($E_{elec}^{cluster}$ + ZPE), Spin Operator (S^2), Energy Difference $\Delta(E_{elec}^{cluster}$ + ZPE), Binding Energy per Atom (E_B), and Binding Energy per Bond (E_{bond})

SM	method	E_{elec}^{Pt} (hartrees)	$E_{elec}^{cluster}$ (hartrees)	ZPE (hartrees)	$E_{elec}^{cluster}$ + ZPE (hartrees)	S^2	$\Delta(E_{elec}^{cluster}$ + ZPE) (kcal/mol)	E_B (eV)	E_{bond} (eV)
1	B3LYP	−119.289064	−477.482762	0.001753	−477.481009		18.18[a]		
	B3PW91	−119.328118	−477.661408	0.001899	−477.659509		18.87[a]		
3	B3LYP	−119.303538	−477.512821	0.001736	−477.511085	2.0160		2.03	1.35
	B3PW91	−119.343853	−477.692805	0.001850	−477.690955	2.0186		2.16	1.44
	BP86		−477.949934	0.001762	−477.948172	2.0044			
5	B3LYP	−119.119751	−477.503749	0.001782	−477.501967	6.0008	5.03[a]		
	B3PW91	−119.165008	−477.684412	0.001892	−477.682520	6.0010	4.43[a]		
3[c]	B3LYP		−477.499404	0.001448	−477.497956	2.0006	7.55[b]	1.94	1.29
	B3PW91		−477.672923	0.001413	−477.671510	2.0007	11.34[b]	2.02	1.35
	BP86		−477.935713	0.002038	−477.933675	2.0001	9.10[b]		

[a] $\Delta(E_{elec}$ + ZPE) = E_{elec} + ZPE (singlet or quintet) − E_{elec} + ZPE(triplet). [b] $\Delta(E_{elec}$ + ZPE) = E_{elec} + ZPE (Pt_4, T_d) − E_{elec} + ZPE(triplet). [c] Pt_4 (T_d): Pt−Pt distances were kept constant and equal to the experimental bulk, 2.775 Å.

or metastable structures of platinum cluster, reported in the literature, nor to establish comparisons between the obtained structures and those reported previously in the literature, since this kind of discussion can be found in refs 9−13, 27, 31, 33, 41, 43, and 87−99 and in references cited therein. Despite the number of tests that have been performed, the results reported in this paper are mainly related to the most stable isomers, including the identification of the optimal states of spin multiplicity and the preferential adsorption sites, as suggested for calculations considering clusters and adsorbates.[7,16−18,27,28,33,41,46,78,87,88,93−96,100−105]

3.1. Pt_4 Cluster. The importance of employing cluster models containing more than one layer was emphasized in a study about the effects of the electric field on the adsorption, charge-transfer, and vibration states in metallic electrodes for systems such as H_2O/Pt(111), H_2O/Pt(100), and $(H_2O)_2$/Pt(111).[106] Consequently, tetrahedral geometries have been used to represent Pt_4 clusters. By employing the interstitial electron model (IEM), Kua and Goddard[41] determined that the ground state of Pt_4 must contain two electrons in a symmetrical combination (ligand) of four 6s orbitals, and therefore, 38 electrons are distributed into 20 5d orbitals, corresponding to a triplet state. In a recent paper about the magnetic and structural stabilities of small transition metal clusters, Futschek et al.[88] also verified that the ground state of the tetrahedral Pt_4 must have a spin multiplicity (SM) equal to 3 (total spin $S = 1$ and SM = 3). Although Lin et al.[46] reported a quintet ground state for the distorted Pt_4 with D_{2d} symmetry, results analogous to those of Futschek et al. can also be found in the literature.[9,26,31,33,43,49,87,94,98]

Geometry optimizations performed without symmetry constraints yielded a distorted tetrahedron (Figure 1) characterized by the absence of imaginary frequencies. The electronic energies ($E_{elec}^{cluster}$) and the energy differences ($\Delta(E_{elec}^{cluster}$ + ZPE)) indicate that the triplet state is the most stable, followed by the quintet and singlet states (Table 1).

In this way, the triplet state is 19−20 kcal/mol^{-1} more stable than the singlet state and approximately 5−6 kcal/mol^{-1} more stable than the quintet state. The Pt_4 cluster (triplet state, symmetry T_d), obtained by keeping the Pt−Pt distances constant (2.775 Å), is 8−12 kcal/mol^{-1} less stable than the distorted tetrahedron. The stabilization resulting from the symmetry reduction is attributed to the Jahn−Teller effect.[10,33,46] Lin et al. verified that the tetrahedron with symmetry D_{2d} is around 7.4 kcal/mol^{-1} more stable than the T_d tetrahedron.[46] It should also be emphasized that an optimization test for the Pt_4 (triplet state) cluster employing the relativistic approximation DKH2 (Douglas−Kroll−Hess second-order scalar relativistic),[107−115] combined with the hybrid functional B3LYP and the ECP MWB, gave a structure with geometric parameters similar to those obtained without this approximation, but at an elevated computational cost.

The binding energy per atom (E_B, Table 1), or atomization energy, was calculated according to eq 1, where E_{elec}^{Pt} and $E_{elec}^{cluster}$ denote the electronic energies for a single platinum atom and for a platinum cluster of N atoms, respectively.[10,11,33]

$$E_B = E_{elec}^{Pt} - (E_{elec}^{cluster}/N) \quad (1)$$

The binding energy per bond (E_{bond}, Table 1) is defined by eq 2 and can provide information about the bond strength in the cluster.[10] In this case, N_{bond} is the total number of bonds.

$$E_{bond} = (NE_{elec}^{Pt} - E_{elec}^{cluster})/N_{bond} \quad (2)$$

The ground state for platinum atoms is a triplet, as observed in Table 1, which is in close agreement with theoretical and experimental data.[33,46,116,117] By considering the triplet electronic state for both the platinum atom and cluster, the atomization energy values, E_B, are in close agreement with those reported by Li and Balbuena (2.17 eV/atom),[33] but are lower than the values reported by Nie et al. (2.554 eV/atom)[11] and by Xiao and Wang (2.68 eV/atom for E_B and 1.79 eV/bond for E_{bond}).[10] In addition, E_B and E_{bond} are smaller for the cluster with symmetry T_d, confirming the increase in energy stabilization when the symmetry is reduced.

3.2. Pt_4−(H_2O, $^{\bullet}OH$, $^{\bullet}H$) Complexes. ***3.2.1. Geometries and Adsorption Energies.*** The adsorption of H_2O, $^{\bullet}OH$, and $^{\bullet}H$ on the platinum cluster, Pt_4, was studied by considering different adsorption sites and spin multiplicities. The results reported here concern the optimal spin state and the most stable adsorption site only.

Geometry optimizations reveal that the adsorbates tend to bind preferably atop of the cluster (Figure 2). For the radical species ($^{\bullet}OH$ and $^{\bullet}H$), the optimal spin multiplicity of the system cluster−adsorbate is a quartet, while for H_2O it is a triplet. Sites of high coordination, such as hollow sites, have been described as the most favorable for hydrogen adsorption on platinum.[8,118] However, calculations have demonstrated that the bond strength is approximately degenerate atop, bridge, and 3-fold-hollow sites;[15,78,118,119] for instance, an energy difference of only 0.1−0.2 eV is observed between the adsorption energies on the top and hollow sites.[118] Considering that hydrogen chemisorption on the Pt(111) surface shows a very flat potential energy surface, although acceptable, the accuracy of the methods based on DFT

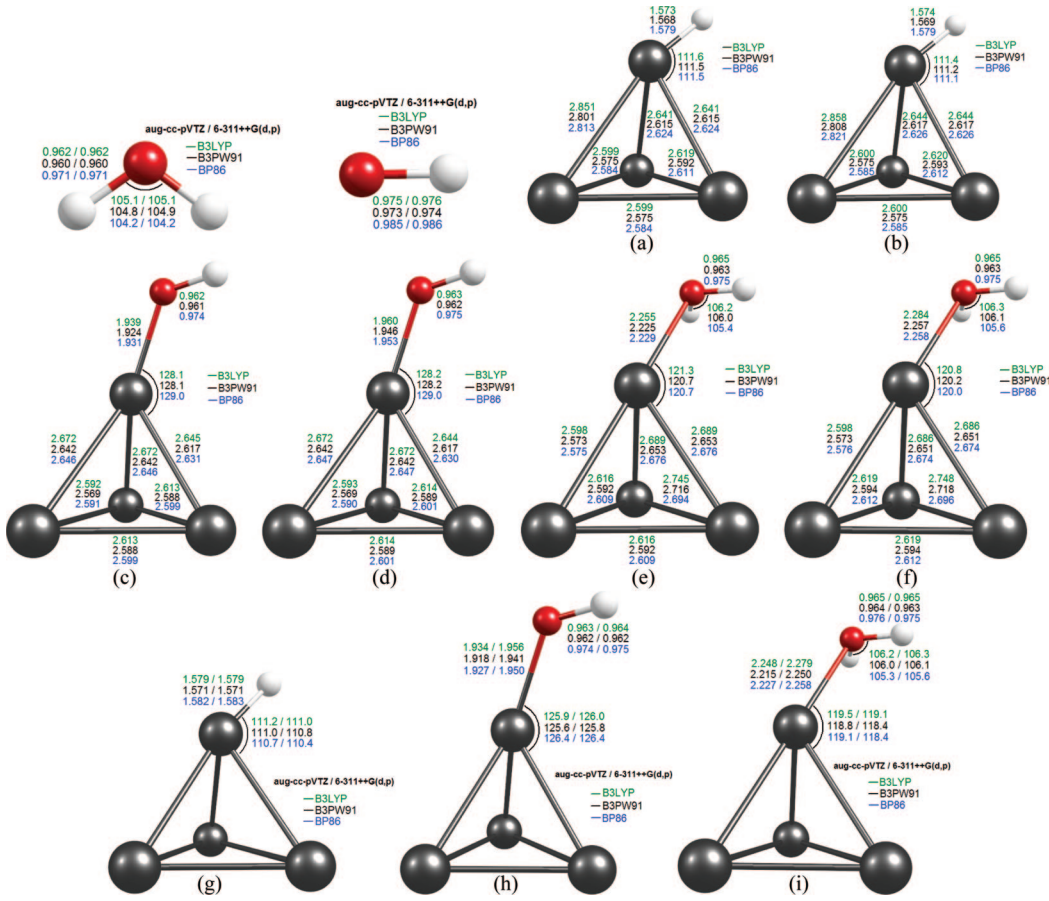

Figure 2. Equilibrium geometries for adsorbates and cluster−adsorbate systems: (a, c, and e) MWB,aug-cc-pVTZ; (b, d, and f) MWB,6-311++G(d,p); (g, h, and i) Pt_4 (T_d, Pt−Pt distance = 2.775 Å). Distances are given in angstroms and angles in degrees.

do not allow for a realistic comparison with experimental data.[78] So theoretical studies considering hydrogen adsorbed on the top or on the other adsorption sites can be found in the literature.[7,8,16,78] As for •OH, the experimental proposal for the 3-fold site bonding is that it should occur only in the situation where an elevated covering of this radical on the metallic surface is observed.[16] Regarding water absorption, the classical model sets forth that, at the solid−liquid interface, the water molecules can assume "oxygen-up" or "oxygen-down" orientations because of the interaction between the electrical field and the dipole moment.[106] Reaching an understanding of the binding site and orientation of the water monomers has stimulated several computational and experimental studies,[120] since the preferential orientation can affect not only the response from the water in the presence of an applied electrochemical field but also its dissociation process. Frequently, it is assumed that the water molecule adsorbs in a way that the O−H bonds are kept distant from the surface, thus maximizing the dipole interactions, which are important for system stabilization.[120] Studies have shown that the water absorption at the atop site[120] as well as on the other sites, with a large degree of coordination,[121] can be observed. Quantum mechanics calculations performed by Jacob and Goddard[122] established that on the completely water-saturated Pt(111) surface half of the water molecules are located almost parallel to the surface, generating Pt−O bonds. The other half are positioned perpendicular to the surface, with their hydrogen atoms pointing toward platinum, thus forming Pt−HO agostic bonds.

The adsorption sites, adsorbate geometries, and the interaction distances presented in Figure 2 are in good agreement with those reported by Jacob,[16] who employed a cluster with 35 platinum atoms, as well as with others.[7,24,118,120,123,124] Thus, in the case of the radicals •OH and •H, the Pt−O and Pt−H bonds should be established by the interaction between unpaired electron spins, one from the adsorbate and the other from the d orbital of the platinum surface.[16] By considering an average value between the different methods and basis set, Pt−O and Pt−H present bond lengths of 1.57 and 1.94 Å, respectively. The water molecule binds to the cluster through the oxygen, in a way that the O−H bonds assume a roughly parallel orientation[6,8,16,120] with respect to the face Pt(1)−Pt(2)−Pt(4). In this case, the average distance observed for the Pt−O bond is ca. 2.25 Å. In general, this sort of interaction occurs between the lone pair of the oxygen atom (which is perpendicular to the molecular plane of water) and the platinum surface, in a donor−acceptor bond, which is followed by a charge transfer from the water molecule to platinum.[16,125] As opposed to the radicals •OH and •H, in the case of the interaction between water and the platinum cluster, the electrons are probably not paired, which should happen if a covalent bond is formed. This can explain the largest Pt−O distance in the case of water.[16]

The Pt−(•OH, H_2O) bond distances are slightly larger when the basis set 6-311++G(d,p) is employed. A comparison between the relaxed structure and the structure that keeps the Pt−Pt distances constant (Pt_4, T_d) shows no significant differences in the cluster−adsorbate distances.

The obtained geometries show a difference regarding the spatial orientation of the adsorbates. For the atomic hydrogen and water molecule, the bond Pt(1)−H,H_2O is aligned with the bond Pt(1)−Pt(3). However, for the hydroxyl radical, the Pt(1)−OH bond is oriented in the same plane containing the Pt(1)−Pt(2) bond (Figure 3).

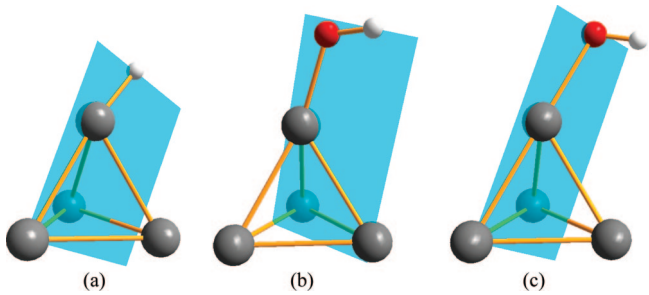

Figure 3. Spatial orientation of the adsorbates: (a) Pt_4-H; (a) Pt_4-OH; (c) Pt_4-H_2O.

As verified in Figures 1 and 2, some Pt−Pt bond lengths are also kept constant even for the relaxed cluster. For instance, the isolated cluster presents four Pt−Pt bonds with the same distance (Pt(1)−Pt(2) = Pt(1)−Pt(4) = Pt(2)−Pt(3) = Pt(3)−Pt(4)). However, the similarity pattern of the bond lengths is not the same for Pt_4-H,H_2O and Pt_4-OH. For the system containing adsorbed hydrogen or water, the similarity pattern is Pt(1)−Pt(2) = Pt(1)−Pt(4) and Pt(2)−Pt(3) = Pt(3)−Pt(4). On the other hand, for systems with the radical OH, the pattern is Pt(1)−Pt(3) = Pt(1)−Pt(4) and Pt(2)−Pt(3) = Pt(2)−Pt(4). The similarity pattern of the Pt−Pt bond distances does not depend on the employed functional.

In relation to the isolated clusters (Figure 1), adsorbate binding leads to structural changes in some Pt−Pt bond lengths. The effect of the adsorbate on the metallic cluster structures, that is, the large reorganization of Pt atoms, was also observed by Calvo and Balbuena in a study about the reactivity of the radical OOH with the clusters Pt_{10}, Pd_{10}, and Pt_xPd_y (x and y = 3 or 7).[105] In this way, the adsorption of the hydrogen atom causes an increase in the Pt(1)−Pt(3) bond length, which is aligned with the Pt−H bond, and a decrease in the Pt(2)−Pt(3), Pt(2)−Pt(4), and Pt(3)−Pt(4) bond lengths. The Pt(1)−Pt(2) and Pt(1)−Pt(4) bond lengths present only slight changes under adsorption. The radical hydroxyl also causes a lengthening of the Pt(1)−Pt(3) bond distance but with small intensity, as observed for the hydrogen radical. On the other hand, a bond shortening of Pt(2)−Pt(3), Pt(2)−Pt(4), and Pt(3)−Pt(4) was observed. For the system Pt_4-H_2O, an increase of Pt(1)−Pt(2) and Pt(1)−Pt(4) was followed by a decrease in all the other Pt−Pt bond lengths. The changes on the bond lengths are quite similar for all functionals. As for the adsorbates, the O−H bond of the radical OH diminishes, while the same bond length (O−H) increases when the water molecule binds to the cluster.

To check the influence of the adsorbates on the stability and strength of the Pt−Pt bonds, E_B and E_{bond} were recalculated (Table 2) by employing the electronic energies of the Pt_4 cluster and by considering the geometries of Pt_4 in the Pt_4-(•H, •OH, H_2O) systems.

Despite the geometric changes described for the Pt−Pt bond distance upon H_2O, •OH, and •H adsorption, the E_B and E_{bond} values are constant; that is, while some Pt−Pt bonds become weaker, others become stronger upon adsorption, so the E_B and E_{bond} values do not change.

The adsorption energy (E_{ads}) on the cluster surface is defined as

$$E_{ads} = E_{elec}^{cluster-adsorbate} - E_{elec}^{cluster} - E_{elec}^{adsorbate} \quad (6)$$

where $E_{elec}^{cluster-adsorbate}$, $E_{elec}^{cluster}$, and $E_{elec}^{adsorbate}$ are the total energy of the complex (cluster + adsorbate), metallic cluster, and adsorbate molecule, respectively.[6,8,123] All adsorption energies are presented in Tables 3 and 4, and they correspond, respectively, to results obtained by using the aug-cc-pVTZ and 6-311++G(d,p) basis set for hydrogen and oxygen atoms.

The •H and •OH radicals strongly bind to the platinum cluster. Despite their similar E_{ads} values, the •OH radical binds slightly more strongly than •H. On the other hand, the E_{ads} of the water molecule is almost 5−6 times smaller than the E_{ads} for the radical species. The E_{ads} values of the •H and •OH radicals for the Pt_4 cluster T_d, with fixed Pt−Pt distances, are slightly lower than the E_{ads} value for the cluster with relaxed structure. Jacob and Goddard performed calculations considering the cluster Pt_{35}, and they demonstrated that the change in the position of the platinum atoms that are not fastened to the surface is less than 3%, suggesting that the relaxation effect is negligible.[28,78] No dependence was observed for the E_{ads} values with the basis set (aug-cc-pVTZ and 6-311++G(d,p)). However, the E_{ads} values are larger when determined by the functional BP86 compared with the B3LYP or B3PW91 functionals. Independent of the computational model employed, the E_{ads} values are overestimated in relation to the experimental values: 0.42 eV for H_2O,[126] 2.60 eV for •OH,[127] and 2.64 eV for •H.[128] Evaluation of the energetic chemisorption of •OH on platinum and the metal−OH bond strength is considered a very tough task. In this case, the experimental values range from 1.0 to 2.6 eV,[19] due the fact that the adsorption of OH is affected by the presence of the coadsorbates.[19,129] Nevertheless, considering the small size of the cluster employed in this work, the theoretical E_{ads} values (especially the values obtained with the model B3LYP/MWB,6-311++G(d,p), Table 4) are in close agreement with the experimental data, indicating that the applied of level theory is able to describe this sort of system with good accuracy. In a study about the reduction of oxygen on platinum cluster (adsorption and decomposition of OOH and H_2O_2), Wang and Balbuena showed that the functional B3LYP is adequate to describe open-shell systems involving platinum cluster and adsorbates.[18] In addition, the calculated E_{ads} are in agreement with the large range of values reported in the literature, which are obtained by considering different descriptions for the platinum surface, cluster size, and adsorption sites,[6−8,15−20,24,78,106,118,120−124,130−135] thus reinforcing the importance of these intermediates in several catalytic processes. Considering only the top of the platinum cluster, different E_{ads} values can be found. For instance, the values for atomic hydrogen range from 2.58 eV (Pt_{10}(7,3)[118]) to 3.02 eV (Pt_{10} planar[78]). For the hydroxyl radical, the values vary from 1.77 to 2.92 eV when the clusters Pt_8 and Pt_3 are employed, respectively.[7,17] Finally, for water adsorption, the values range from 0.27 (by using the three layer slabs approximation[130]) to 1.02 eV (on Pt_3 cluster[17]). It should be mentioned that by reporting these values, our intention is neither to cover all previously published results nor to establish limits for acceptable values of E_{ads} for H_2O, •OH, and •H on platinum (atop site), since the systematic search can include new values to the above-mentioned ones. In addition, Ramaker et al.[47] have published in 2003 a table which contains the most recent theoretical and experimental results for the adsorption of •H, •O, and •OH on platinum.

3.2.2. Vibrational Frequencies. The changes in the stretching frequencies can be interpreted as a direct consequence of the structural perturbations.[136] Table 5 presents the stretching normal modes for the O−H bonds from water and the hydroxyl radical.

After adsorption, a blue shift is observed for the O−H stretching of the hydroxyl radical due to the decrease in the O−H bond length. For the water molecule, the symmetric and the asymmetric stretching modes indicate a small red shift (the O−H bond lengths of water are slightly increased after

TABLE 2: Spin Multiplicity (SM), Electronic Energy of the Cluster ($E_{elec}^{cluster}$) in the gGeometry of the Cluster−Adsorbate System, Binding Energy per Atom (E_B), and Binding Energy per Bond (E_{bond})

SM	geometry		$E_{elec}^{cluster}$ (hartrees)	E_B (eV)	E_{bond} (eV)
3	Pt_4 in the geometry of the Pt_4-H_2O system	Figure 2e, B3LYP	−477.512212	2.03	1.35
		Figure 2f, B3LYP	−477.512282	2.03	1.35
		Figure 2e, B3PW91	−477.692247	2.16	1.44
		Figure 2f, B3PW91	−477.692307	2.16	1.44
	Pt_4 in the geometry of the Pt_4-OH system	Figure 2c, B3LYP	−477.510603	2.02	1.34
		Figure 2d, B3LYP	−477.510628	2.02	1.34
		Figure 2c, B3PW91	−477.690335	2.14	1.43
		Figure 2d, B3PW91	−477.690368	2.14	1.43
	Pt_4 in the geometry of the Pt_4-H system	Figure 2a, B3LYP	−477.512197	2.03	1.35
		Figure 2b, B3LYP	−477.512146	2.03	1.35
		Figure 2a, B3PW91	−477.692234	2.16	1.44
		Figure 2b, B3PW91	−477.692179	2.15	1.44

TABLE 3: Spin Multiplicity (SM), System Electronic Energy (E_{elec}^{system}), Zero Point Correction (ZPE), System Electronic Energy Corrected by ZPE (E_{elec}^{system} + ZPE), Adsorption Energies (E_{ads}), and Adsorption Energies Corrected by ZPE (E_{ads} + ZPE)

computational model	system	SM	E_{elec}^{system} (hartrees)	ZPE (hartrees)	E_{elec}^{system} + ZPE (hartrees)	$\|E_{ads}\|$ (eV)	$\|E_{ads}$ + ZPE$\|$ (eV)
B3LYP/MWB,aug-cc-pVTZ	•H	2	−0.502260		−0.502260		
	•OH	2	−75.768599	0.008413	−75.760185		
	H_2O	1	−76.466198	0.021240	−76.444959		
	Pt_4-H	4	−478.126636	0.008754	−478.117883	3.04	2.84
	Pt_4-OH	4	−553.395807	0.014693	−553.381114	3.11	2.99
	Pt_4-H_2O	3	−553.997534	0.026194	−553.971340	0.50	0.42
	Pt_4-H^a	4	−478.111346	0.008119	−478.103227	2.98	2.80
	Pt_4-OH^a	4	−553.380669	0.014182	−553.366487	3.07	2.95
	$Pt_4-H_2O^a$	3	−553.985987	0.025653	−553.960334	0.55	0.47
B3PW91/MWB,aug-cc-pVTZ	•H	2	−0.504068		−0.504068		
	•OH	2	−75.737192	0.008491	−75.728701		
	H_2O	1	−76.436029	0.021399	−76.414630		
	Pt_4-H	4	−478.308957	0.008957	−478.300000	3.05	2.86
	Pt_4-OH	4	−553.547550	0.014947	−553.532602	3.20	3.07
	Pt_4-H_2O	3	−554.148965	0.026556	−554.122409	0.55	0.46
	Pt_4-H^a	4	−478.287499	0.008192	−478.279307	3.01	2.82
	Pt_4-OH^a	4	−553.525478	0.014310	−553.511168	3.14	3.02
	$Pt_4-H_2O^a$	3	−554.131420	0.025894	−554.105526	0.61	0.53
BP86/MWB,aug-cc-pVTZ	•H	2	−0.500146		−0.500146		
	•OH	2	−75.764009	0.008148	−75.755861		
	H_2O	1	−76.466174	0.020636	−76.445538		
	Pt_4-H	4	−478.567465	0.008705	−478.558760	3.19	3.00
	Pt_4-OH	4	−553.845659	0.014364	−553.831294	3.58	3.46
	Pt_4-H_2O	3	−554.439316	0.025637	−554.413679	0.63	0.54
	Pt_4-H^a	4	−478.549144	0.007958	−478.541187	3.08	2.92
	Pt_4-OH^a	4	−553.827072	0.013781	−553.813291	3.46	3.37
	$Pt_4-H_2O^a$	3	−554.424528	0.024998	−554.399530	0.62	0.55

[a] Pt_4 (T_d): Pt−Pt distances were kept constant and equal to the experimental bulk, 2.775 Å.

adsorption). On the basis of experimental and theoretical data, Thiel[125] reported that, among the characteristics related to the adsorption of water on metallic surfaces, the interaction of water with the surface must cause only small perturbations (regarding the bond lengths, bond angle, and vibrational frequencies of water) in comparison with the values observed in the gas phase.

3.2.3. Charge Transfer. In several situations, the quantity of electron density transferred from a donor to an acceptor is small, ca. mille-electrons, but these small charges have a fundamental role in the properties of both subsystems. For the studied systems, the charge transfer (CT; Table 6) is significant for both the full-optimized geometries and the structures where the Pt−Pt distances were kept constant. In Pt_4-H and Pt_4-OH, CT takes place from the cluster toward the adsorbates, while for the Pt_4-H_2O the opposite situation is observed.[16,125] This indicates that the platinum−adsorbate binding depends on the nature of the adsorbate.

Jacob reported a CT of 0.28e from the water to the cluster Pt_{35}.[16] By employing the clusters Pt_{10} and Pt_{13} as models of the metallic electrodes Pt(111) and Pt(100), respectively, Ohwaki et al.[106] analyzed the effects of the electric field (EF) on the charge transfer, vibrational states, and geometric orientation of the water molecules (monomer and dimer) adsorbed on the platinum surface. They observed that when EF = 0 or EF > 0, the charge transfer from the water molecule to the platinum predominates, and in this case the water is adsorbed at the top site. On the other hand, if EF < 0, the interaction between the dipole moment of the water and the electric field dominates over the charge transfer. By considering EF = 0, the authors verified that the magnitude of the interaction energy between the water (adsorbed on the top site) and the platinum surface is larger for Pt(111) (≈0.56 eV) than for Pt(100) (≈0.43 eV). This observation was explained in terms of the energy levels of the platinum 6s orbitals, which are more elevated for Pt(100).[106] The best agreement between the calculated and experimental data were obtained by using the model B3LYP/MWB,6-311++G(d,p); for that reason the following analyses will discuss the results obtained with this model.

TABLE 4: Spin Multiplicity (SM), System Electronic Energy (E_{elec}^{system}), Zero Point Correction (ZPE), System Electronic Energy Corrected by ZPE (E_{elec}^{system} + ZPE), Adsorption Energies (E_{ads}), and Adsorption Energies Corrected by ZPE (E_{ads} + ZPE)

computational model	system	SM	E_{elec}^{system} (hartrees)	ZPE (hartrees)	E_{elec}^{system} + ZPE (hartrees)	$\|E_{ads}\|$ (eV)	$\|E_{ads}$ + ZPE$\|$ (eV)
B3LYP/MWB,6-311++G(d,p)	•H	2	−0.502257		−0.502257		
	•OH	2	−75.762412	0.008447	−75.753965		
	H_2O	1	−76.458532	0.021283	−76.437249		
	Pt_4−H	4	−478.125484	0.008786	−478.116698	3.00	2.81
	Pt_4−OH	4	−553.385086	0.014670	−553.370416	2.99	2.87
	Pt_4−H_2O	3	−553.990194	0.026318	−553.963876	0.51	0.42
	Pt_4−H[a]	4	−478.110303	0.008146	−478.102157	2.96	2.77
	Pt_4−OH[a]	4	−553.369997	0.014149	−553.355847	2.94	2.83
	Pt_4−H_2O[a]	3	−553.978705	0.025780	−553.952926	0.56	0.48
B3PW91/MWB,6-311++G(d,p)	•H	2	−0.504065		−0.504065		
	•OH	2	−75.730720	0.008525	−75.722195		
	H_2O	1	−76.428219	0.021447	−76.406772		
	Pt_4−H	4	−478.307623	0.008984	−478.298638	3.01	2.82
	Pt_4−OH	4	−553.536079	0.014929	−553.521150	3.06	2.94
	Pt_4−H_2O	3	−554.141176	0.026689	−554.114487	0.55	0.46
	Pt_4−H[a]	4	−478.286373	0.008220	−478.278154	2.98	2.79
	Pt_4−OH[a]	4	−553.514068	0.014279	−553.499790	3.00	2.89
	Pt_4−H_2O[a]	3	−554.123695	0.026037	−554.097657	0.61	0.53
BP86/MWB,6-311++G(d,p)	•H	2	−0.500141		−0.500141		
	•OH	2	−75.757941	0.008181	−75.749760		
	H_2O	1	−76.458649	0.020681	−76.437968		
	Pt_4−H	4	−478.566221	0.008731	−478.557490	3.16	2.97
	Pt_4−OH	4	−553.835057	0.014345	−553.820713	3.46	3.34
	Pt_4−H_2O	3	−554.431740	0.025802	−554.405939	0.63	0.54
	Pt_4−H[a]	4	−478.548070	0.007981	−478.540089	3.05	2.89
	Pt_4−OH[a]	4	−553.816539	0.013753	−553.802786	3.34	3.25
	Pt_4−H_2O[a]	3	−554.417052	0.025173	−554.391879	0.62	0.55

[a] Pt_4 (T_d): Pt−Pt distances were kept constant and equal to the experimental bulk, 2.775 Å.

TABLE 5: Vibrational Frequencies (cm^{-1})

		system					
			Pt_4−OH			Pt_4−H_2O	
computational model	mode description	•OH	Pt_4	Pt_4(T_d)	H_2O	Pt_4	Pt_4(T_d)
B3LYP/MWB,aug-cc-pVTZ	O−H stretch	3693	3815	3807			
	H−O−H symmetric stretch				3797	3761	3759
	H−O−H asymmetric stretch				3899	3853	3850
	H−O−H bend				1627	1619	1618
B3LYP/MWB,6-311++G(d,p)	O−H stretch	3708	3833	3826			
	H−O−H symmetric stretch				3817	3788	3786
	H−O−H asymmetric stretch				3922	3883	3881
	H−O−H bend				1603	1619	1619
B3PW91/MWB,aug-cc-pVTZ	O−H stretch	3727	3846	3835			
	H−O−H symmetric stretch				3829	3787	3783
	H−O−H asymmetric stretch				3934	3880	3875
	H−O−H bend				1630	1619	1618
B3PW91/MWB,6-311++G(d,p)	O−H stretch	3742	3864	3855			
	H−O−H symmetric stretch				3851	3814	3811
	H−O−H asymmetric stretch				3959	3911	3908
	H−O−H bend				1605	1621	1621
BP86/MWB,aug-cc-pVTZ	O−H stretch	3577	3674	3664			
	H−O−H symmetric stretch				3680	3627	3623
	H−O−H asymmetric stretch				3785	3718	3714
	H−O−H bend				1593	1575	1575
BP86/MWB,6-311++G(d,p)	O−H stretch	3591	3693	3684			
	H−O−H symmetric stretch				3701	3657	3654
	H−O−H asymmetric stretch				3810	3753	3750
	H−O−H bend				1567	1576	1577

3.2.4. Spin Density. In the hydroxyl radical, the unpaired electron is preferentially located at the oxygen atom, in a p_π lone-pair-like orbital. The adsorption of •OH radical on the platinum cluster causes a redistribution of the spin density (obtained by the Mulliken population analysis, Table 7), which is characterized by an abrupt decrease in the spin density at oxygen and a sharing of this density between the platinum atoms. An analogous conclusion is obtained for the adsorption of atomic hydrogen. In this way, an increase in the spin density for all platinum atoms is observed, mainly at Pt(1), Pt(2), and Pt(4). The spin density re-distribution suggests that the electronic structure of the adsorbates is largely affected after adsorption. The changes in spin densities at platinum atoms after water absorption are not intense. In contrast with radical adsorption, the spin density of all Pt atoms does not change.

TABLE 6: Charge Transfer, CT (e)

	$Pt_4 \rightarrow H$		$Pt_4 \rightarrow OH$		$H_2O \rightarrow Pt_4$	
computational model	Pt_4-H	$Pt_4(T_d)-H$	Pt_4-OH	$Pt_4(T_d)-OH$	Pt_4-H_2O	$Pt_4(T_d)-H_2O$
B3LYP/MWB,6-31++G(d,p)	0.117	0.120	0.340	0.316	0.139	0.143
B3PW91/MWB,6-31++G(d,p)	0.081	0.076	0.326	0.293	0.176	0.183
BP86/MWB,6-31++G(d,p)	0.079	0.080	0.258	0.230	0.203	0.209

TABLE 7: Spin Densities Obtained by the Mulliken Population Analysis at B3LYP/MWB,6-311++G(d,p)

atom	Pt_4	$Pt_4(T_d)$	Pt_4-H	$Pt_4(T_d)-H$	Pt_4-OH	$Pt_4(T_d)-OH$	Pt_4-H_2O	$Pt_4(T_d)-H_2O$
Pt(1)	0.59	0.56	0.87	0.91	0.86	0.90	0.58	0.58
Pt(2)	0.41	0.44	0.73	0.68	0.68	0.64	0.44	0.46
Pt(3)	0.59	0.56	0.61	0.66	0.64	0.62	0.54	0.50
Pt(4)	0.41	0.44	0.73	0.68	0.64	0.62	0.44	0.46
H(Pt)			0.06	0.07				
O(Pt)					0.18	0.21	0.01	0.02
H(O)					0.00	0.00	0.00	0.00

3.2.5. Molecular Orbitals. The singly occupied molecular orbitals, SOMOs, of the systems Pt_4-H and Pt_4-OH present a large overlap region located at the metal−adsorbate interaction sites, corroborating the large adsorption energies of these systems (Figure 4a,d).

However, the same does not happen in the case of the complex Pt_4-H_2O (Figure 4j), in which the overlap region is observed for SOMO-1 (Figure 4k). The lone pairs of the oxygen atom in water have a smaller contribution to the metal−adsorbate bonding than the lone pairs of the oxygen in the •OH radical.

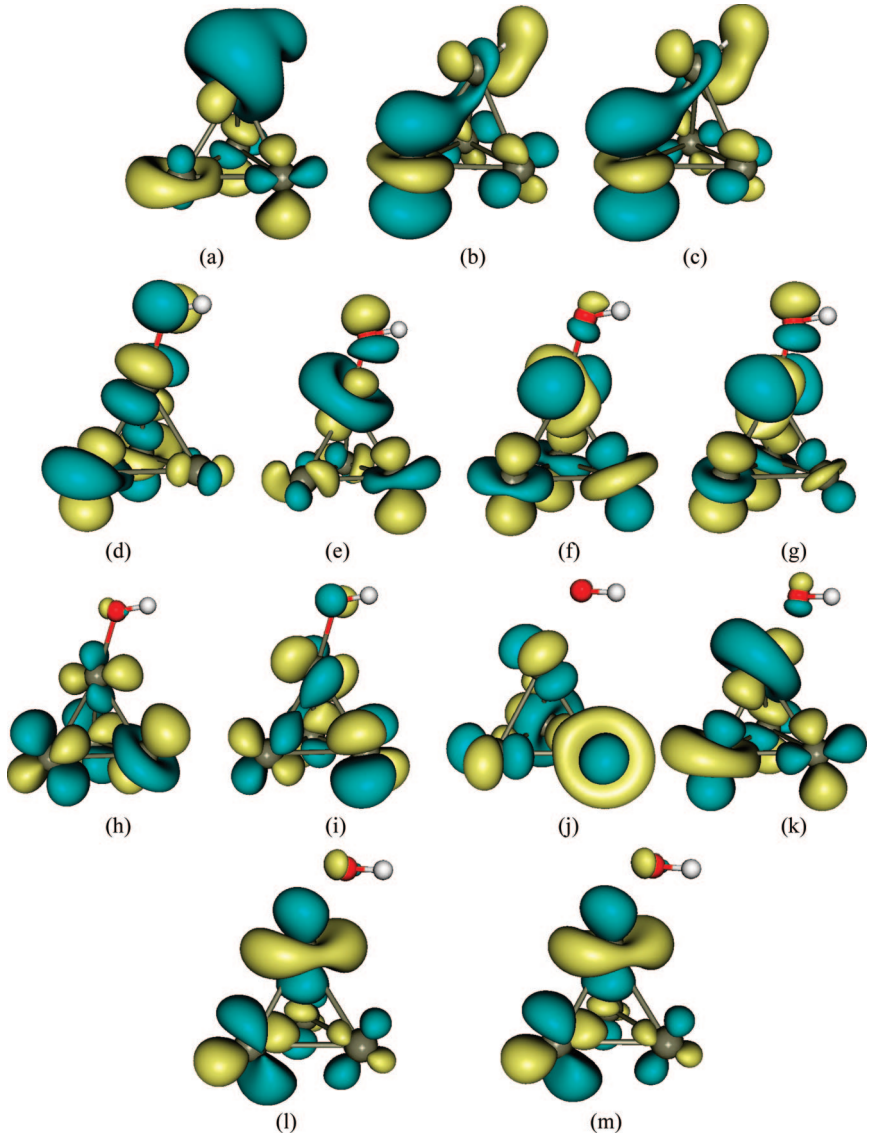

Figure 4. Molecular orbitals: (a) SOMO Pt_4-H; (b) SOMO-5 (α spin) Pt_4-H; (c) SOMO-5 (β spin) Pt_4-H; (d) SOMO Pt_4-OH; (e) SOMO-1 Pt_4-OH; (f) SOMO-3 (α spin) Pt_4-OH; (g) SOMO-3 (β spin) Pt_4-OH; (h) SOMO-6 (α spin) Pt_4-OH; (i) SOMO-6 (β spin) Pt_4-OH; (j) SOMO Pt_4-H_2O; (k) SOMO-1 Pt_4-H_2O; (l) SOMO-10 (α spin) Pt_4-H_2O; (m) SOMO-10 (β spin) Pt_4-H_2O.

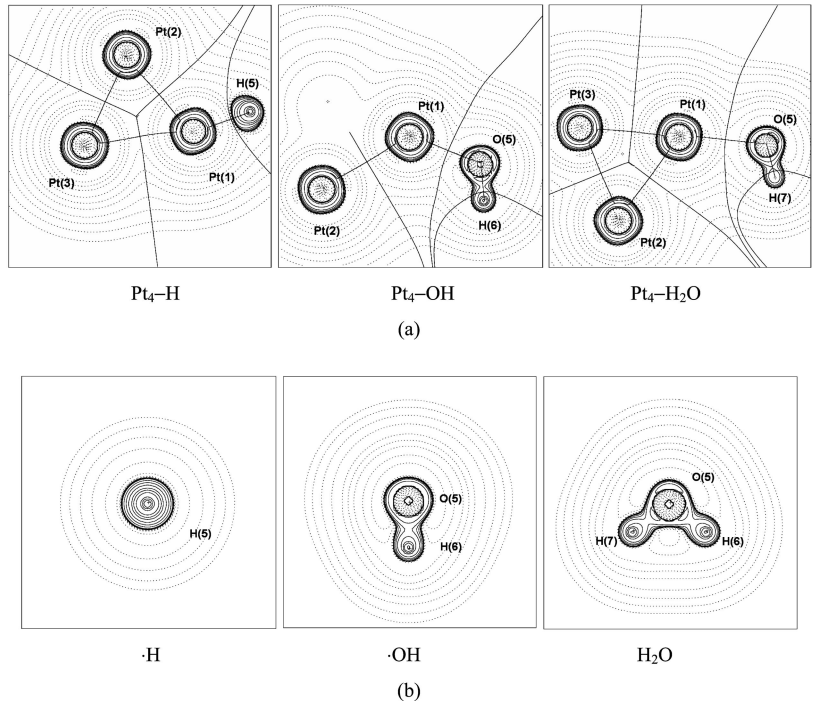

Figure 5. Contour-line diagrams of the Laplacian distribution $\nabla^2\rho(r)$ of (a) Pt_4−adsorbate complexes and (b) isolated ligands ·H, ·OH, and H_2O at UB3LYP/MWB,6-311++G(d,p). Dashed lines indicate local charge depletion ($\nabla^2\rho_b > 0$), and solid lines indicate local charge concentration ($\nabla^2\rho_b < 0$). The solid lines connecting the atomic nuclei are the bond paths, and the solid lines separating the atomic nuclei indicate the zero-flux surfaces in the molecular plane. The crossing points of the bond paths and zero-flux surfaces are the bond critical points.

TABLE 8: Bond Critical Point Properties (a.u.) of Complexes 1−4 at UB3LYP/MWB,6-311++G(d,p)

compounds	BCPs	ρ_b[a]	$\nabla^2\rho_b$	ε	G_b	V_b	H_b	$-G_b/V_b$
Pt_4	Pt(1)−Pt(2)	0.066	0.128	0.030	0.051	−0.070	−0.019	0.729
	Pt(1)−Pt(3)	0.068	0.127	0.022	0.052	−0.072	−0.020	0.722
	Pt(1)−Pt(4)	0.066	0.128	0.030	0.051	−0.070	−0.019	0.729
	Pt(2)−Pt(3)	0.066	0.128	0.030	0.051	−0.070	−0.019	0.729
	Pt(2)−Pt(4)	0.052	0.117	0.044	0.040	−0.051	−0.011	0.784
	Pt(3)−Pt(4)	0.066	0.128	0.030	0.051	−0.070	−0.019	0.729
Pt_4−H	Pt(1)−Pt(2)	0.066	0.125	0.045	0.050	−0.068	−0.018	0.735
	Pt(1)−Pt(3)	0.043	0.104	0.007	0.033	−0.040	−0.007	0.825
	Pt(1)−Pt(4)	0.066	0.125	0.045	0.050	−0.068	−0.018	0.735
	Pt(1)−H(5)	0.163	−0.030	0.007	0.102	−0.212	−0.110	0.481
	Pt(2)−Pt(3)	0.071	0.129	0.025	0.054	−0.076	−0.022	0.711
	Pt(2)−Pt(4)	0.068	0.128	0.032	0.052	−0.073	−0.021	0.712
	Pt(3)−Pt(4)	0.071	0.129	0.025	0.054	−0.076	−0.022	0.711
Pt_4−OH	Pt(1)−Pt(2)	0.066	0.125	0.022	0.050	−0.069	−0.019	0.725
	Pt(1)−Pt(3)	0.063	0.109	0.053	0.045	−0.062	−0.017	0.726
	Pt(1)−Pt(4)	0.063	0.109	0.053	0.045	−0.062	−0.017	0.726
	Pt(1)−O(5)	0.132	0.583	0.025	0.184	−0.222	−0.038	0.829
	Pt(2)−Pt(3)	0.069	0.130	0.037	0.053	−0.074	−0.021	0.716
	Pt(2)−Pt(4)	0.069	0.130	0.037	0.053	−0.074	−0.021	0.716
	Pt(3)−Pt(4)	0.072	0.136	0.042	0.056	−0.079	−0.023	0.709
	O(5)−H(6)	0.362	−2.434	0.007	0.076	−0.761	−0.685	0.100
·OH	O(1)−H(2)	0.358	−2.410	0.044	0.070	−0.742	−0.672	0.094
Pt_4−H_2O	Pt(1)−Pt(2)	0.060	0.124	0.054	0.047	−0.063	−0.016	0.746
	Pt(1)−Pt(3)	0.072	0.114	0.021	0.051	−0.074	−0.023	0.689
	Pt(1)−Pt(4)	0.060	0.124	0.054	0.047	−0.063	−0.016	0.746
	Pt(1)−O(5)	0.058	0.279	0.007	0.074	−0.079	−0.005	0.937
	Pt(2)−Pt(3)	0.068	0.130	0.031	0.053	−0.073	−0.020	0.726
	Pt(2)−Pt(4)	0.054	0.121	0.055	0.043	−0.055	−0.022	0.782
	Pt(3)−Pt(4)	0.068	0.130	0.031	0.053	−0.073	−0.020	0.726
	O(5)−H(6)	0.361	−2.549	0.019	0.066	−0.769	−0.703	0.086
	O(5)−H(7)	0.361	−2.549	0.019	0.066	−0.769	−0.703	0.086
H_2O	O(1)−H(2)	0.366	−2.491	0.026	0.075	−0.773	−0.698	0.097
	O(1)−H(2)	0.366	−2.491	0.026	0.075	−0.773	−0.698	0.097

[a] One atomic unit of $\rho_b = 6.748$ e Å^{-3}, of $\nabla^2\rho_b = 24.10$ e Å^{-5}, and of energy $= e_2/a_0 = 627.51$ kcal/mol $= 27.21$ eV.

Other molecular orbitals such as SOMO-5 of Pt_4−H (Figure 4b,c); SOMO-1, SOMO-3, and SOMO-6 of Pt_4−OH (Figures 4e−i); and SOMO-10 of Pt_4−H_2O (Figure 4l,m) also exhibit lobes in the metal−adsorbate binding region.

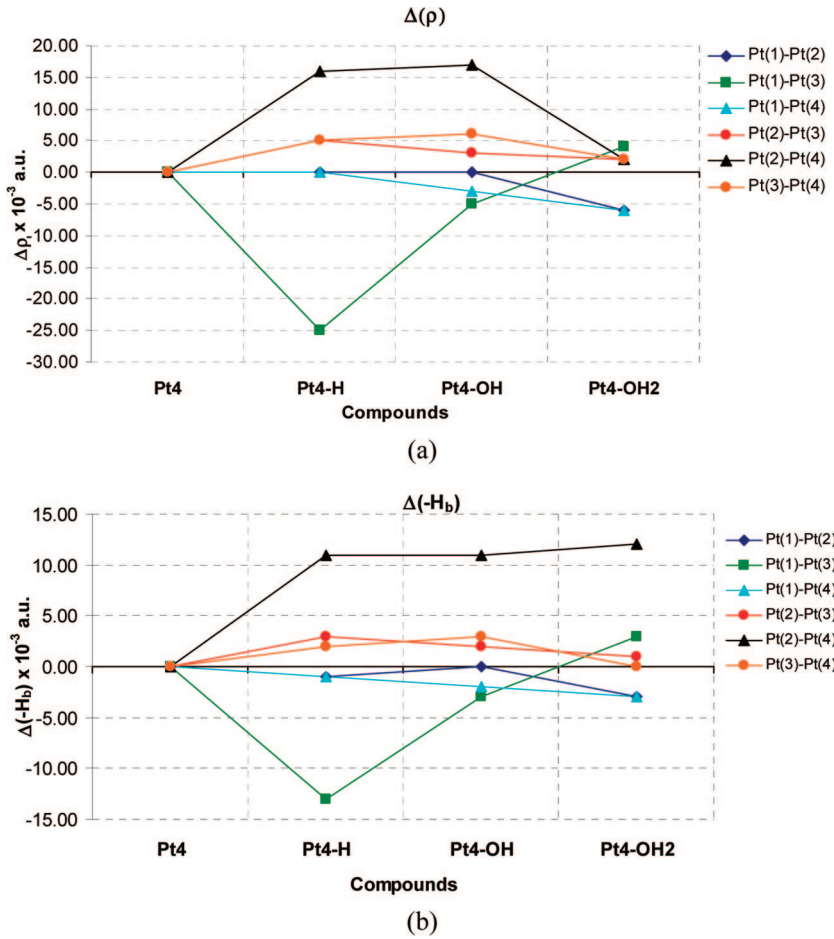

Figure 6. Variations in the bond critical point properties, ρ_b and H_b, of $Pt_4-(H,OH,H_2O)$ complexes.

3.2.6. Analysis of the Electron Density — QTAIM. The charge distribution in the Pt_4, Pt_4-H, Pt_4-OH, and Pt_4-H_2O compounds (obtained by full optimization) was analyzed by the AIM method, developed by Bader and co-workers.[79,80] Figure 5 shows the contour lines diagram of the Laplacian of the electron density, $\nabla^2\rho(r)$, in the plane containing the adsorbates. For the Pt_4−adsorbate complexes, the Laplacian shape in the vicinity of the terminal Pt(1)−H(5) and Pt(1)−O(5) interactions shows a circular form at Pt(1), while the ligand atoms (H(5) and O(5)) exhibit a somewhat distorted shape with the charge concentration ($\nabla^2\rho(r) < 0$, solid lines) region pointing toward Pt(1).

Comparing Figure 5a,b, we notice that the latter distortion is very large for H(5) and very small for O(5), which is directly related with the local hardness and softness of H and O. No distortion of the Laplacian distribution was observed for the Pt atoms, independent of the spin multiplicity of the complex under consideration. Analysis of the Laplacian distribution indicates that in all the interactions the bond critical points, BCPs, connecting the cluster−adsorbate are located in regions of charge depletion, suggesting that these interactions are closed-shell-like. However, according to Cremer and Kraka,[137] the Laplacian is not so reliable to describe covalent interactions. In addition, the results indicate that the visual inspection of the Laplacian distribution is not so sensitive to explore this class of bonding interactions, either.

More information about the AIM analysis can be obtained from the numerical data, which are given in Table 8. According to Bader,[80] an electron-sharing (covalent) bond is characterized by a negative value of the Laplacian at the bond critical point ($\nabla^2\rho_b$), while closed-shell interactions (ionic bonds and van der Waals bonds) have positive $\nabla^2\rho_b$ values. The result in Table 8 would then suggest that all bonds analyzed by AIM are ionic, except for Pt(1)−H, O(5)−H(6), and O(5)−H(7) in complexes Pt_4-H, Pt_4-OH, and Pt_4-H_2O, respectively. As already pointed out by Cremer and Kraka,[137] the total energy density at the BCP, H_b, is a better criterion to estimate the covalent character of a chemical interaction.[79,138,139]

The virial theorem in the BCP (au) can be expressed as

$$(1/4)\nabla^2\rho_b = 2G_b + V_b \qquad (7)$$

and relates the $\nabla^2\rho_b$ with the kinetic (G_b, always positive) and potential (V_b, always negative) energy densities. The total energy density, H_b, is given by the sum of G_b and V_b.

$$H_b = G_b + V_b \qquad (8)$$

The H_b sign will depend on which contribution, potential or kinetic, prevails in the BCP locally. $H_b < 0$ reflects the prevalence of the potential energy density and is a consequence of the stabilization of the accumulated electronic charge, a typical property of covalent interactions.[140,141] Therefore, a partial covalent character is attributed to interactions with $H_b < 0$. It is worth mentioning that $\nabla^2\rho_b$ remains small and positive, which is a characteristic of closed-shell interactions, since, in eq 8, $|V_b| > G_b$, but, in eq 7, $|V_b| < 2G_b$.[140,142] A positive H_b value suggests closed-shell interactions (ionic bonds and van der Waals bonds).

The $-G_b/V_b$ ratio was also proposed as an indicator of the nature of a given interaction.[143] This ratio must be higher than

1 for noncovalent interactions and lower than 0.5 in the case of covalent interactions (shared interactions). $-G_b/V_b$ values lying between 0.5 and 1 indicate partially covalent interactions. According to Table 8, all bonds, in particular Pt−Pt, exhibit some covalent character. A considerable covalent character is observed for Pt(1)−H(5) (−0.110 au) compared with Pt(1)−O(5) in the Pt_4−OH complex, while, for the Pt_4-H_2O system, H_b is roughly zero. The latter interactions exhibit also an increase in the electron density at the BCP, ρ_b (0.163 au for Pt(1)−H(5) in Pt_4−H and 0.132 au for Pt(1)−O(5) in Pt_4−OH). However, for Pt(1)−O(5) in the Pt_4-H_2O complex, either ρ_b or H_b is very small, suggesting that the interaction between the platinum cluster and water is much more ionic than the same interaction between the cluster and the radicals •H and•OH. Analogous conclusions can be obtained by using the $-G_b/V_b$ ratio. The topological parameters correlate very well with the structural changes upon adsorption. These geometrical changes can also be correlated with the covalent character; that is, in the case of Pt_4−H the Pt(1)−Pt(3) bond has decreased covalent character compared with the isolated Pt_4 cluster (Figure 6a,b).

The AIM numerical data suggest that the complexation between Pt_4 and the •H radical is much more covalent than the interactions involving •OH and H_2O. Figure 6 makes the behavior of ρ_b and H_b in Pt−Pt chemical bonds upon complexation clear. According to Figure 6, Pt(1)−Pt(3) chemical bond has decreased electron density and covalent character upon complexation with •H or •OH, while, upon complexation with H_2O, ρ_b is kept roughly constant and H_b increases for the Pt(2)−Pt(4) bond.

4. Conclusions

The changes in the chemical bonds, structure, and electron density of the Pt_4 cluster and the adsorbates were employed to characterize the nature of the Pt_4−adsorbates (H, •OH, and H_2O) interactions. All calculations were performed by using the density functional theory (B3LYP, B3PW91, and BP86) in conjunction with the effective core potential MWB for platinum atoms and the 6-311++G(d,p) and aug-cc-pVTZ basis set for H and O atoms. Identification of the optimal state of spin multiplicity and the preferential adsorption sites was also performed. The electronic energies indicated that the triplet state of Pt_4 is most stable, followed by the quintet and singlet states. The small stability (8−12 kcal.mol^{-1}) of the Pt_4 cluster with T_d symmetry in relation to the relaxed cluster (distorted tetrahedron) is attributed to the Jahn−Teller effect, which is also verified by the E_B and E_{bond} values.

The adsorbates bind preferentially at the atop site of the cluster, yielding complexes cluster−adsorbate in the triplet (Pt_4-H_2O) and quartet (Pt_4−H and Pt_4−OH) states. The equilibrium geometries exhibit some differences in terms of the adsorbate orientation; that means, Pt(1)−H and $Pt(1)-H_2O$ are aligned with the Pt(1)−Pt(3) bond, while Pt(1)−OH superimposes the Pt(1)−Pt(2) bond. The adsorption of •H causes an increase in the Pt(1)−Pt(3) bond distance. Despite the structural changes in Pt_4, both E_B and E_{bond} remain constant, thus representing a balance between the Pt−Pt bonds that become weak and those that become strong.

The •H and •OH radicals bind to the platinum surface 5 or 6 times more strongly than the H_2O. The symmetry effects (relaxation of the Pt_4 geometry) do not affect the adsorption energies, which are close to the experimental data, mainly those obtained by using the model B3LYP/MWB,6-311++G(d,p). Adsorption is followed by a charge transfer from the Pt_4 cluster toward the adsorbate, but this charge transfer occurs in a reversed way when the adsorbate is H_2O. The adsorption of the radicals •H and •OH on platinum causes a remarkable redistribution of the spin density, characterized by a density sharing between the •H and •OH radicals and the Pt_4 cluster. This effect is not observed in the case of water adsorption, and the spin density remains constant. Analysis of the singly occupied molecular orbitals, SOMOs, indicates an overlap region between the metal−adsorbate bonds in Pt_4−H and Pt_4−OH. The contributions of the oxygen lone pairs of the water molecule to the metal−adsorbate bond are smaller than those observed for the •OH radical.

Finally, the covalent character of the cluster−adsorbate interactions, determined by the topological analysis of the electron density, reveals the following tendency: Pt_4−H > Pt_4−OH > Pt_4-H_2O. The $-G_b/V_b$ ratio indicates that Pt_4−H has a covalent character, Pt_4−OH is partially covalent, and Pt_4-H_2O is almost noncovalent. The topological analysis of the electron density is also in good agreement with the structural changes in the cluster.

Acknowledgment. The authors thank FAPESP, CNPq and CAPES for financial support. R.L.T.P. thanks FAPESP for the postdoctoral research fellowship (Grant No. 2006/06035-7). G.F.C. thanks FAPESP for a postdoctoral scholarship (Grant No. 2007/04379-3). F.H. thanks financial support from FAPESP (Grant No. 05/00106-7), CNPq (Grant No. 550581/2005-7 and Grant No. 555436/2006-3), and IMMP/MCT. S.E.G. thanks CNPq for a research scholarship (Grant No. 302014/2004-7). The authors also acknowledge Ali Faiez Taha for technical support and LCCA-USP for the generous allocation of computational resources.

Supporting Information Available: Complete ref 50 and the *x*, *y*, *z* coordinates and thermochemistry for the studied compounds. This material is available free of charge via the Internet at http://pubs.acs.org.

References and Notes

(1) (a) Vielstich, W. *Fuel Cells*; Wiley Interscience: Bristol, U.K., 1965. (b) Vielstich, W.; Iwasita, T. In *Handbook of Heterogeneous Catalysis*; Ertl, G., Knözinger, H., Weitkamp, J., Eds.; Verlag Chemie: Weinheim, Germany, 1997; Vol. 4, p 2090.

(2) Iwasita, T. *J. Braz. Chem. Soc.* **2002**, *13*, 401.

(3) Lizcano-Valbuena, W. H.; de Azevedo, D. C.; Gonzalez, E. R. *Electrochim. Acta* **2004**, *49*, 1289.

(4) Casado-Rivera, E.; Volpe, D. J.; Alden, L.; Lind, C.; Downie, C.; Vázquez-Alvarez, T.; Angelo, A. C. D.; DiSalvo, F. J.; Abruña, H. D. *J. Am. Chem. Soc.* **2004**, *126*, 4043.

(5) Hayase, M.; Kawase, T.; Hatsuzawa, T. *Electrochem. Solid-State Lett.* **2004**, *7*, A231.

(6) Perez, A.; Vilkas, M. J.; Cabrera, C. R.; Ishikawa, Y. *J. Phys. Chem. B* **2005**, *109*, 23571.

(7) Kua, J.; Goddard, W. A., III *J. Am. Chem. Soc.* **1999**, *121*, 10928.

(8) Ishikawa, Y.; Diaz-Morales, R. R.; Perez, A.; Vilkas, M. J.; Cabrera, C. R. *Chem. Phys. Lett.* **2005**, *411*, 404.

(9) Rubio, J.; Zurita, S.; Barthelat, J. C.; Illas, F. *Chem. Phys. Lett.* **1994**, *217*, 283.

(10) Xiao, L.; Wang, L. *J. Phys. Chem. A* **2004**, *108*, 8605.

(11) Nie, A.; Wu, J.; Zhou, C.; Yao, S.; Luo, C.; Forrey, R. C.; Cheng, H *Int. J. Quantum Chem.* **2007**, *107*, 219.

(12) Zhang, W.; Xiao, L.; Hirata, Y.; Pawluk, T.; Wang, L. *Chem. Phys. Lett.* **2004**, *383*, 67.

(13) Majumdar, D.; Dai, D.; Balasubramanian, K. *J. Chem. Phys.* **2000**, *113*, 7928.

(14) Chen, L.; Cooper, A. C.; Pez, G. P.; Cheng, H. *J. Phys. Chem. C* **2007**, *111*, 5514.

(15) Desai, S. K.; Neurock, M.; Kourtakis, K. *J. Phys. Chem. B* **2002**, *106*, 2559.

(16) Jacob, T. *Fuel Cells* **2006**, *6*, 159.

(17) Balbuena, P. B.; Altomare, D.; Vadlamani, N.; Bingi, S.; Agapito, L. A.; Seminario, J. M. *J. Phys. Chem. A* **2004**, *108*, 6378.

(18) Wang, Y.; Balbuena, P. B. *J. Chem. Theory Comput.* **2005**, *1*, 935.
(19) Michaelides, A.; Hu, P. *J. Am. Chem. Soc.* **2001**, *123*, 4235, and references cited therein.
(20) Michaelides, A.; Hu, P. J. *Chem. Phys.* **2001**, *114*, 513.
(21) Hyman, M. P.; Medlin, J. W. *J. Phys. Chem. B* **2005**, *109*, 6304.
(22) Bernardo, C. G. P. M.; Gomes, J. A. N. F. *J. Mol. Struct. (THEOCHEM)* **2001**, *542*, 263.
(23) Bernardo, C. G. P. M.; Gomes, J. A. N. F. *J. Mol. Struct. (THEOCHEM)* **2002**, *582*, 159.
(24) Ishikawa, Y.; Liao, M.-S.; Cabrera, C. R. *Surf. Sci.* **2000**, *463*, 66.
(25) Watwe, R. M.; Spiewak, B. E.; Cortright, R. D.; Dumesic, J. A. *Catal. Lett.* **1998**, *51*, 139.
(26) Cruz, A.; Bertin, V.; Poulain, E.; Benítez, J. I.; Castillo, S. *J. Chem. Phys.* **2004**, *120*, 6222.
(27) Jacob, T.; Muller, R. P.; Goddard, W. A., III *J. Phys. Chem. B* **2003**, *107*, 9465.
(28) Jacob, T.; Goddard, W. A., III *J. Phys. Chem. B* **2005**, *109*, 297.
(29) Minot, C.; Markovits, A. *J. Mol. Struct. (THEOCHEM)* **1998**, *424*, 119.
(30) Watwe, R. M.; Cortright, R. D.; Nørskov, J. K.; Dumesic, J. A. *J. Phys. Chem. B* **2000**, *104*, 2299.
(31) Poulain, E.; Benítez, J. I.; Castillo, S.; Bertin, V.; Cruz, A. *J. Mol. Struct. (THEOCHEM)* **2004**, *709*, 67.
(32) Xia, F.; Cao, Z. *J. Phys. Chem. A* **2006**, *110*, 10078.
(33) Li, T.; Balbuena, P. B. *J. Phys. Chem. B* **2001**, *105*, 9943.
(34) García-Hernández, M.; Curulla, D.; Clotet, A.; Illas, F. *J. Chem. Phys.* **2000**, *113*, 364.
(35) Curulla, D.; Clotet, A.; Ricart, J. M.; Illas, F. *Electrochim. Acta* **1999**, *45*, 639.
(36) Teliska, M.; Murthi, V. S.; Mukerjee, S.; Ramaker, D. E. *J. Electrochem. Soc.* **2005**, *152*, A2159.
(37) Wasileski, S. A.; Weaver, M. J. *Faraday Discuss.* **2002**, *121*, 285.
(38) Illas, F.; Rubio, J. *J. Chem. Phys.* **1996**, *105*, 7192.
(39) Chen, M.; Bates, S. P.; van Santen, R. A.; Friend, C. M. *J. Phys. Chem. B* **1997**, *101*, 10051.
(40) Illas, F.; Zurita, S.; Marquez, A. M.; Rubio, J. *Surf. Sci.* **1997**, *376*, 279.
(41) Kua, J.; Goddard, W. A., III *J. Phys. Chem. B* **1998**, *102*, 9481.
(42) Illas, F.; Zurita, S.; Rubio, J.; Marquez, A. M. *Phys. Rev. B* **1995**, *52*, 12372.
(43) Endou, A.; Ohashi, N.; Yoshizawa, K.; Takami, S.; Kubo, M.; Miyamoto, A.; Broclawik, E. *J. Phys. Chem. B* **2000**, *104*, 5110.
(44) Akinaga, Y.; Taketsugu, T.; Hirao, K. J. *Chem. Phys.* **1997**, *107*, 415.
(45) Fahmi, A.; van Santen, R. A. Z. *Z. Phys. Chem.* **1996**, *197*, 203.
(46) Lin, X.; Ramer, N. J.; Rappe, A. M.; Hass, K. C.; Schneider, W. F.; Trout, B. L. *J. Phys. Chem. B* **2001**, *105*, 7739.
(47) Ramaker, D. E.; Teliska, M.; Zhang, Y.; Stakheev, A. Yu.; Koningsberger, D. C *Phys. Chem. Chem. Phys.* **2003**, *5*, 4492.
(48) Oudenhuijzen, M. K.; van Bokhoven, J. A.; Ramaker, D. E.; Koningsberger, D. C. *J. Phys. Chem. B* **2004**, *108*, 20247.
(49) Xiao, L.; Wang, L. *J. Phys. Chem. B* **2007**, *111*, 1657.
(50) Frisch, M. J.; *Gaussian 03*, Revision A.1; Gaussian Inc.: Pittsburgh, PA, 2003.
(51) Becke, A. D. *J. Chem. Phys.* **1993**, *98*, 5648.
(52) Lee, C.; Yang, W.; Parr, R. G. *Phys. Rev. B* **1988**, *37*, 785.
(53) Miehlich, B.; Savin, A.; Stoll, H.; Preuss, H. *Chem. Phys. Lett.* **1989**, *157*, 200.
(54) Burke, K.; Perdew, J. P.; Wang, Y. In *Electronic Density Functional Theory: Recent Progress and New Directions*; Dobson, J. F., Vignale, G. , Das, M. P., Eds.; Plenum: New York, 1998.
(55) Perdew, J. P. In *Electronic Structure of Solids*; Ziesche, P., Eschrig, H., Eds.; Akademie Verlag: Berlin, 1991.
(56) Perdew, J. P.; Burke, K.; Wang, Y. *Phys. Rev. B* **1996**, *54*, 16533.
(57) Perdew, J. P. *Phys. Rev. B* **1986**, *33*, 8822.
(58) Becke, A. D. *Phys. Rev. A* **1988**, *38*, 3098.
(59) Schwerdtfeger, P.; Dolg, M.; Schwarz, W. H. E.; Bowmaker, G. A.; Boyd, P. D. W. *J. Chem. Phys.* **1989**, *91*, 1762.
(60) Andrae, D.; Haeussermann, U.; Dolg, M.; Stoll, H.; Preuss, H. *Theor. Chim. Acta* **1990**, *77*, 123.
(61) Kuechle, W.; Dolg, M.; Stoll, H.; Preuss, H. *Mol. Phys.* **1991**, *74*, 1245.
(62) Bergner, A.; Dolg, M.; Kuechle, W.; Stoll, H.; Preuss, H. *Mol. Phys.* **1993**, *80*, 1431.
(63) Leininger, T.; Nicklass, A.; Stoll, H.; Dolg, M.; Schwerdtfeger, P. *J. Chem. Phys.* **1996**, *105*, 1052.
(64) Fuentealba, P.; Preuss, H.; Stoll, H.; Szentpaly, L. v. *Chem. Phys. Lett.* **1989**, *89*, 418.
(65) Kaupp, M.; Schleyer, P. v. R.; Stoll, H.; Preuss, H. *J. Chem. Phys.* **1991**, *94*, 1360.
(66) Dolg, M.; Stoll, H.; Preuss, H.; Pitzer, R. M. *J. Phys. Chem.* **1993**, *97*, 5852.
(67) Dolg, M.; Wedig, U.; Stoll, H.; Preuss, H. *J. Chem. Phys.* **1987**, *86*, 866.
(68) Dolg, M.; Stoll, H.; Preuss, H. *Theor. Chim. Acta* **1993**, *85*, 441.
(69) Igel-Mann, G.; Stoll, H.; Preuss, H. *Mol. Phys.* **1988**, *65*, 1321.
(70) Cao, X. Y.; Dolg, M. *J. Mol. Struct. (THEOCHEM)* **2002**, *581*, 139.
(71) Nicklass, A.; Dolg, M.; Stoll, H.; Preuss, H. *J. Chem. Phys.* **1995**, *102*, 8942.
(72) Krishnan, R.; Binkley, J. S.; Seeger, R.; Pople, J. A. *J. Chem. Phys.* **1980**, *72*, 650.
(73) McLean, A.D.; Chandler, G. S *J. Chem. Phys.* **1980**, *72*, 5639.
(74) Clark, T.; Chandrasekhar, J.; Spitznagel, G. W.; Schleyer, P. v. R. *J. Comput. Chem.* **1983**, *4*, 294.
(75) Kendall, R. A., Jr.; Harrison, R. J. *J. Chem. Phys.* **1992**, *96*, 6796.
(76) Herzberg, G. Electronic Spectra and Electronic Structure of Polyatomic Molecules. *Molecular Spectra and Molecular Structure*, Vol. 3; D. Van Nostrand: New York, 1966.
(77) Kittel, C. In *Introduction to Solid-State Physics*, 4th ed.; Wiley: New York, 1986.
(78) Psofogiannakis, G.; St-Amant, A.; Ternan, M. *J. Phys. Chem. B* **2006**, *110*, 24593.
(79) Bader, R. F. W. *Atoms in Molecules. A Quantum Theory*; Oxford University Press: Oxford, U.K., 1990.
(80) Bader, R. F. W. *Chem. Rev.* **1991**, *91*, 893.
(81) Bader, R. F. W. *J. Phys. Chem. A* **1998**, *102*, 7314.
(82) (a) Hobza, P.; Sponer, J.; Cubero, E.; Orozco, M.; Luque, F. J. *J. Phys. Chem. B* **2000**, *104*, 6286. (b) Popelier, P. L. A. *J. Phys. Chem. A* **1998**, *102*, 1873. (c) Caramori, G. F.; Frenking, G. *Organometallics* **2007**, *26*, 5815. (d) Caramori, G. F.; Galembeck, S. E. *J. Phys. Chem. A* **2007**, *111*, 1705. (e) Caramori, G. F.; de Oliveira, K. T.; Galembeck, S. E.; Bultinck, P.; Constantino, M. G. *J. Org. Chem.* **2007**, *72*, 76. (f) Matta, C. F.; Gillespie, R. J. *J. Chem. Educ.* **2002**, *79*, 1141. (g) Bader, R. F. W.; Matta, C. F. *Inorg. Chem.* **2001**, *40*, 5603. (h) Matta, C. F.; Arabi, A. A.; Keith, T. A. *J. Phys. Chem. A* **2007**, *111*, 8864.
(83) Biegler-König, F.; Bader, R. F. W.; Tang, T. H. J. *J. Comput. Chem.* **1982**, *3*, 317.
(84) Flükiger, P.; Lüthi, H. P.; Portmann, S.; Weber, J. MOLEKEL: An Interactive Molecular Graphics Tool, 2000−2002. *CHIMIA*; Portmann, S., Lüthi, H. P., Eds.; Swiss Center for Scientific Computing: Manno, Switzerland, 2000; Vol. 54, p 766.
(85) Zhurko, G. A.; Zhurko, D. A. Chemcraft Lite, http://www.chemcraftprog.com.
(86) *DIAMOND-Crystal and Molecular Structure Visualization*, Demonstration Version 3.1f, Crystal Impact; K. Brandenburg & H. Putz GbR: Bonn, Germany, 2008.
(87) Tian, W. Q.; Ge, M.; Sahu, B. R.; Wang, D.; Yamada, T.; Mashiko, S. *J. Phys. Chem. A* **2004**, *108*, 3806.
(88) Futschek, T.; Hafner, J.; Marsman, M. *J. Phys.: Condens. Matter* **2006**, *18*, 9703.
(89) Huda, M. N.; Niranjan, M. K.; Sahu, B. R.; Kleinman, L. *Phys. Rev. A* **2006**, *73*, 053201.
(90) Yang, S. H.; Drabold, D. A.; Adams, J. B.; Ordejón, P.; Glassford, K. *J. Phys.: Condens. Matter* **1997**, *9*, L39.
(91) Wang, L.-L.; Khare, S. V.; Chirita, V.; Johnson, D. D.; Rockett, A. A.; Frenkel, A. I.; Mack, N. H.; Nuzzo, R. G. *J. Am. Chem. Soc.* **2006**, *128*, 131.
(92) Aprà, E.; Carter, E. A.; Fortunelli, A. *Int. J. Quantum Chem.* **2004**, *100*, 277.
(93) Tian, W. Q.; Ge, M.; Gu, F.; Aoki, Y. *J. Phys. Chem. A* **2005**, *109*, 9860.
(94) Xu, Y.; Shelton, W. A.; Schneider, W. F. *J. Phys. Chem. A* **2006**, *110*, 5839.
(95) Zhanpeisov, N. U.; Fukumura, H. *J. Chem. Theory Comput.* **2006**, *2*, 801.
(96) Ankudinov, A. L.; Rehr, J. J.; Low, J. J.; Bare, S. R. *J. Chem. Phys.* **2002**, *116*, 1911.
(97) Balasubramanian, K. *J. Chem. Phys.* **1987**, *87*, 6573.
(98) Dai, D.; Balasubramanian, K. *J. Chem. Phys.* **1995**, *103*, 648.
(99) Majumdar, D.; Dai, D.; Balasubramanian, K. *J. Chem. Phys.* **2000**, *113*, 7919.
(100) Dimakis, N.; Iddir, H.; Díaz-Morales, R. R.; Liu, R.; Bunker, G.; Chung, E.-H.; Smotkin, E. S. *J. Phys. Chem. B* **2005**, *109*, 1839.
(101) Balbuena, P. B.; Calvo, S. R.; Lamas, E. J.; Salazar, P. F.; Seminario, J. M. *J. Phys. Chem. B* **2006**, *110*, 17452.
(102) Miura, T.; Kobayashi, H.; Domen, K. *J. Phys. Chem. B* **2000**, *104*, 6809.
(103) Saeys, M.; Reyniers, M.-F.; Neurock, M.; Marin, G. B. *J. Phys. Chem. B* **2003**, *107*, 3844.
(104) Lu, G.; Lan, J.; Li, C.; Wang, W.; Wang, C. *J. Phys. Chem. B* **2006**, *110*, 24541.
(105) Calvo, S. R.; Balbuena, P. B. *Surf. Sci.* **2007**, *601*, 165.

(106) Ohwaki, T.; Kamegai, K.; Yamashita, K. *Bull. Chem. Soc. Jpn.* **2001**, *74*, 1021.
(107) Douglas, M.; Kroll, N. M. *Ann. Phys.* **1974**, *82*, 89.
(108) Hess, B. A. *Phys. Rev. A* **1985**, *32*, 756.
(109) Hess, B. A. *Phys. Rev. A* **1986**, *33*, 3742.
(110) Jansen, G.; Hess, B. A. *Phys. Rev. A* **1989**, *39*, 6016.
(111) de Jong, W. A.; Harrison, R. J.; Dixon, D. A. *J. Chem. Phys.* **2001**, *114*, 48.
(112) Barysz, M.; Sadlej, A. J. *J. Mol. Struct. (THEOCHEM)* **2001**, *573*, 181.
(113) Visscher, L.; Dyall, K. G. *At. Data Nuclear Data Tables* **1997**, *67*, 207.
(114) Reiher, M. *Theor. Chem. Acc.* **2006**, *116*, 241.
(115) Peralta, J. E.; Uddin, J.; Scuseria, G. E. *J. Chem. Phys.* **2005**, *122*, 084108.
(116) Benitez, J. I.; Castillo, S.; Poulain, E.; Bertin, V. *J. Chem. Phys.* **2006**, *124*, 024703.
(117) Moore, C. E. In *Natational Bureau of Standards Circular 467*; Keiths, C. C., Ed.; U.S. GPO: Washington, DC, 1971.
(118) Au, C.-T.; Zhou, T.-J.; Lai, W.-J. *Catal. Lett.* **1999**, *62*, 147.
(119) Papoian, G.; Nørskov, J. K.; Hoffmann, R. *J. Am. Chem. Soc.* **2000**, *122*, 4129.
(120) Michaelides, A.; Ranea, V. A.; de Andres, P. L.; King, D. A *Phys. Rev. Lett.* **2003**, *90*, 216102; and references cited therein.
(121) (a) Anderson, A. B. *Surf. Sci.* **1981**, *105*, 159. (b) Sophr, E.; Heinzinger, K. *Chem. Phys. Lett.* **1986**, *123*, 218.
(122) Jacob, T.; Goddard, W. A., III *J. Am. Chem. Soc.* **2004**, *126*, 9360.
(123) Ishikawa, Y.; Liao, M.-S.; Cabrera, C. R. *Surf. Sci.* **2002**, *513*, 98.
(124) Koper, M. T. M.; Shubina, T. E.; van Santen, R. A. *J. Phys. Chem. B* **2002**, *106*, 686.
(125) Thiel, P. A. *Surf. Sci. Rep.* **1987**, *7*, 211.
(126) Sexton, B. A.; Hughes, A. E. *Surf. Sci.* **1984**, *140*, 227.
(127) Anton, A. B.; Cadogan, D. C. *Surf. Sci.* **1990**, *239*, L548.
(128) Gdowski, G. E.; Fair, J. A.; Madix, R. J. *Surf. Sci.* **1983**, *127*, 541.
(129) Patrito, E. M.; Paredas Olivera, P.; Sellers, H. *Surf. Sci.* **1994**, *306*, 447.
(130) Kandoi, S.; Gokhale, A. A.; Grabow, L. C.; Dumesic, J. A.; Mavrikakis, M. *Catal. Lett.* **2004**, *93*, 93.
(131) Greeley, J.; Mavrikakis, M. *J. Am. Chem. Soc.* **2004**, *126*, 3910.
(132) Gong, X.-Q.; Hu, P.; Raval, R. *J. Chem. Phys.* **2003**, *119*, 6324.
(133) Shubina, T. E.; Hartnig, C.; Koper, M. T. M. *Phys. Chem. Chem. Phys.* **2004**, *6*, 4215.
(134) Seong, S.; erson, A. B. *J. Phys. Chem.* **1996**, *100*, 11744.
(135) Bockris, J. O'M.; Abdu, R. *J. Electroanal. Chem.* **1998**, *448*, 189.
(136) (a) Parreira, R. L. T.; Galembeck, S. E. *J. Mol. Struct. (THEOCHEM)* **2006**, *760*, 59. (b) Parreira, R. L. T.; Galembeck, S. E.; Hobza, P. *ChemPhysChem* **2007**, *8*, 87. (c) Parreira, R. L. T.; Valdés, H.; Galembeck, S. E. *Chem. Phys.* **2006**, *331*, 96. (d) Parreira, R. L. T.; Galembeck, S. E. *J. Am. Chem. Soc.* **2003**, *125*, 15614.
(137) Cremer, D.; Kraka, E. *Angew. Chem., Int. Ed. Engl.* **1984**, *23*, 627.
(138) Popelier, P. L. A. *Atoms in Molecules: An Introduction*; Pearson Education: Edinburgh Gate, Harlow, England, 2000.
(139) Gálvez, O.; Gómez, P. C.; Pacios, L. F. *J. Chem. Phys.* **2003**, *118*, 4878.
(140) Arnold, W. D.; Oldfield, E. *J. Am. Chem. Soc.* **2000**, *122*, 12835.
(141) Pacios, L. F. *J. Phys. Chem. A* **2004**, *108*, 1177.
(142) Vorobyov, I.; Yappert, M. C.; DuPré, D. B. *J. Phys. Chem. A* **2002**, *106*, 10691.
(143) Ziółkowski, M.; Grabowski, S. J.; Leszczynski, J. *J. Phys. Chem. A* **2006**, *110*, 6514.

JP8033177